Journal of Bioscience and Bioengineering
VOL. 127 No. 1, 38–44, 2019

www.elsevier.com/locate/jbiosc

Optimization of a dual-functional biocatalytic system for continuous hydrolysis of lactose in milk

Heng Li,[1,3] Yuting Cao,[2] Shuai Li,[3] Yun Jiang,[2] Jianqi Chen,[2] and Zhuofu Wu[2,*]

Computer Science Department, Information and Technology College, Jilin Agricultural University, Changchun 130118, PR China,[1] Jilin Province Innovation Platform of Straw Comprehensive Utilization Technology College of Life Science, Jilin Agricultural University, Changchun 130118, PR China,[2] and Key Laboratory for Molecular Enzymology and Engineering of the Ministry of Education, College of Life Sciences, Jilin University, Changchun 130012, PR China[3]

Received 9 February 2018; accepted 10 July 2018
Available online 8 August 2018

In this study, an amino-functionalized silica matrix encapsulating β-galactosidase was first synthesized in situ, with subsequent covalent anchoring of lysozyme to the outer part of the amino-grafted matrix. Fourier transform infrared (FTIR) spectra verified that β-galactosidase was successfully encapsulated. Meanwhile, the co-immobilized enzymes were demonstrated to retain suitable enzymatic activities and outstanding operational stability during successive reaction cycles. Furthermore, when used for lactose removal from skim milk, the packed-bed column system achieved both a high lactose hydrolysis rate and microbial inactivation ratio during 30 days of continuous operation. Notably, this system exhibited favorable stability during 60 days of continuous hydrolysis of lactose in solution and thus may be appropriate for further development for use in industrial lactose removal from milk.

[**Key words:** β-Galactosidase; Lysozyme; Immobilized enzymes; Co-immobilization; Continuous operating system]

β-Galactosidase, a hydrolase (EC 3.2.1.23) that cleaves the galactosidic linkage of lactose to yield glucose and galactose, holds great promise for the preparation of low lactose milk (1,2). Nevertheless, the utilization of β-galactosidase in the dairy industry has been limited due to the enzyme's poor stability and high cost (3). Because proper immobilization techniques have been used to efficiently overcome such obstacles in other applications (4–9), the encapsulation of β-galactosidase within a support matrix using a fish-in-net method was evaluated here. The results demonstrated that β-galactosidase encapsulation prevented enzyme leakage from the silica matrix due to the larger size of β-galactosidase molecules relative to the matrix pore size. In addition, because silica matrices possess good hydrothermal stability, high mechanical stability and resistance to biodegradation, silica matrix-encapsulated β-galactosidase exhibited excellent stability and reusability (10). However, these advantages were countered by negative effects posed by bacterial colonization of milk during lactose removal. Such a high microbial contamination risk underscores the importance of addressing microbial food safety hazards and spoilage issues that arise during processing of fluid milk (11). Such challenges must be overcome before lactose hydrolysis can be achieved effectively in milk using encapsulated β-galactosidase.

One solution to the microbial contamination problem utilizes lysozyme, an important antimicrobial protein found in mammalian milk and colostrum (12–14). Although the lysozyme content in cow's milk is relatively low, its counterpart in egg white is very abundant (15,16). In our previous work, egg white lysozyme was employed as the antimicrobial agent for use in inhibiting bacterial growth (17). Lysozyme lyses bacterial cells by specifically cleaving the β-1,4 glycosidic linkage between *N*-acetylglucosamine and *N*-acetylmuramic acid in bacterial cell walls (18). Because steric hindrance can affect enzyme effectiveness, lysozyme was anchored to the outer part of the silica support through a covalent linkage to eliminate steric hindrance between lysozyme and bacterial cell walls.

It is well known that stability of enzymes can be enhanced through the use of a glutaraldehyde immobilization method (19–21). Therefore, in this study covalent linkages between the amino groups of the silica matrix and lysozyme were formed via the Schiff's base reaction, with glutaraldehyde acting as a cross-linking reagent (22). In addition to its role in covalent bonding to lysozyme, the amino group on the surface of the silica matrix can be protonated to promote adsorption of lysozyme, while also reducing the pore size of the silica matrix to prevent β-galactosidase leakage from the matrix (23). For this reason, in our earlier research the silica matrix was grafted with aminopropyl groups using a simple co-condensation protocol employing tetraethyl orthosilicate (TEOS) and (3-aminopropyl) triethoxysilane (APTES) that also achieved entrapment of β-galactosidase (17). In addition, because the pores of the amino-silica matrix were blocked by triblock copolymer P123 during covalent attachment, lysozyme could be preferentially tethered to the external surface of the amino-grafted silica via glutaraldehyde crosslinking. Subsequently, after covalent attachment of lysozyme was complete, the P123 in the pore could then be extracted using a washing step to subsequently facilitate the mass transfer of lactose, glucose and galactose within the matrix. When tested in the laboratory, this system of co-immobilized enzymes was observed to provide favorable hydrolytic and

* Corresponding author. Tel./fax: +86 431 84532942.
E-mail address: wzf@jlau.edu.cn (Z. Wu).

1389-1723/$ – see front matter
https://doi.org/10.1016/j.jbiosc.2018.07.009

antimicrobial activities during enzymatic removal of lactose from milk (17). Here we extend our previous work to evaluate this system's performance in continuous operation after first optimizing β-galactosidase encapsulation and lysozyme coupling protocols to optimize enzyme activities. More specifically, immobilization parameters of both the encapsulation of β-galactosidase and the covalent coupling of lysozyme were evaluated to obtain optimal enzymatic activities. Meanwhile, Fourier transform infrared (FTIR) analysis was employed to evaluate the presence of β-galactosidase within the silica matrix, while N_2 adsorption–desorption isotherms were measured to determine the pore size of the silica support.

Finally, activity assays and reuse assessments for co-immobilized β-galactosidase and lysozyme were implemented. Most importantly, the activities of co-immobilized enzymes within the packed-bed reactor were assessed for lactose hydrolysis in skim milk or a lactose solution (Fig. 1).

MATERIALS AND METHODS

Materials β-Galactosidase from *Aspergillus oryzae* (with activity ≥14,000 U/g) was purchased from Amano Enzyme Inc. (Nagoya, Japan). Tetraethyl orthosilicate (TEOS) and Pluronic P123 ($EO_{20}PO_{70}EO_{20}$, *M*av = 5800) and 4-methylumbelliferyl β-D-*N*,*N*′,*N*″-triacetylchitotrioside [4-MU-β-$(GlcNAc)_3$] were supplied by Sigma–Aldrich (St. Louis, MO, USA). 3-Aminopropyltriethoxysilane (APTES) was obtained from Fluka (Buchs, Switzerland). Lysozyme was purchased from Amresco (Solon, OH, USA). The glucose oxidase–peroxidase kit was purchased from Beijing BHKT Clinical Reagent Co., Ltd. (Beijing, China). All other chemicals and reagents were of analytical grade. All aqueous solutions were prepared with Milli-Q water. *Micrococcus lysodeikticus* ATCC 4698 cells were purchased from Sigma–Aldrich.

Pretreatment of β-galactosidase and fabrication of preformed precursors β-Galactosidase was entrapped within an amino functionalized silica matrix through an improved fish-in-net immobilization technique (10). During the process of molecular imprinting, the mixed solution containing 25 ml of lactose solution (37.5%, w/w) and 150 ml of β-galactosidase solution was incubated in liquid nitrogen for 20 min then the frozen mixture was immediately lyophilized. Synthesis of preformed precursors was performed as follows: TEOS (20 g) and 5.4 g of APTES were mixed with 50 g of ethanol and 9.0 g of HCl (0.1 M) with stirring for 2 h, followed by the addition of 30 g of ethanol containing 8.4 g of P123. The mixture was incubated at 25°C for 72 h with stirring to evaporate the ethanol in the solution. Next, 20 g of glycerol was added to the synthesis system and self-assembly of preformed precursors (28–30 g) in the glycerol solution was carried out at 25°C.

Optimization of encapsulation conditions For preparation of matrix-encapsulated β-galactosidase, powdered enzyme (0–2.0 g) imprinted by its natural substrate was added to a mixture containing 20 g of precursors and subjected to magnetic stirring accompanied by dropwise addition of 5 ml of PBS buffer (0.05 M, pH 7.0). A hydrogel formed after the encapsulation system was incubated at 4°C for 4 h. Next, hydrogel was continually aged at 4°C for various amounts of time ranging from 9 to 90 h to sufficiently form a xerogel. Next, an aliquot of xerogel was washed with PBS buffer (0.05 M, pH 7.0) at 4°C in order to extract the polymeric surfactant (P123) and the Bradford method was used to determine the encapsulation yield of β-galactosidase for each sample (24). Encapsulation yields were measured by subtracting the amount of β-galactosidase encapsulated in the matrix from the amount withdrawn in the collected supernatant and rinsing fractions. The formula used for calculation of immobilization yields of β-galactosidase was as follows.

$$Y_1 = \frac{W_1 - W_2}{W_1} \times 100\% \quad (1)$$

where Y_1 is the immobilization yield of β-galactosidase, W_1 is the amount of β-galactosidase incorporated and W_2 is the amount of β-galactosidase in the collected supernatant and the rinsing fractions.

The remainder of the xerogel was stored in 4°C and was used to covalently bind lysozyme in the next procedure. Optimal encapsulation conditions were determined within the following ranges of parameters: (i) a β-galactosidase amount of 0–2.0 g and (ii) aging time of 9–90 h.

Characterization of the matrix N_2 adsorption–desorption isotherms of NH_2-silica-enzymes and NH_2-silica were measured using ASAP 2020 (Micromeritics, Norcross, GA, USA) at 77 K after degassing at 100°C for 12 h. The Brunauer–Emmett–Teller specific surface areas of products were calculated within the relative pressure range $P/P_0 = 0.05$ to 0.3. The Barrett–Joyner–Halenda pore size distribution curve was plotted to determine the pore size of the silica matrix. The FTIR spectrum was recorded using a Thermo Nicolet 5700 spectrometer (Nicolet, Madison, WI, USA) with a resolution of 4 cm^{-1} using the KBr method.

Optimization of the glutaraldehyde coupling procedure Glutaraldehyde (4 mL, 0.02%–10.0%) was added to xerogel with encapsulated β-galactosidase (200 mg) and the mixture was incubated at 25°C with stirring for 2 h. Next, distilled water was used to wash the resulting material several times. Meanwhile, lysozyme was dissolved in various buffers with pH values ranging from 5.0 to 10.0. Precipitates of xerogel coupled with β-galactosidase were harvested by centrifugation and were suspended in 10 mL of lysozyme solutions of various pH values (pH 5.0–10.0) with various lysozyme concentrations (0–2.0 mg/ml). Next, these covalent binding formulations were placed at 4°C for variable amounts of time (1–15 h) and were stored under refrigeration after three washes with buffer. Immobilization yields of lysozyme were determined via the Bradford method (24). The formula used to calculate immobilization yields of lysozyme was as follows.

$$Y_2 = \frac{W_3 - (W_4 - W_2)}{W_3} \times 100\% \quad (2)$$

where Y_2 is the immobilization yield of lysozyme, W_3 is the amount of lysozyme incorporated and W_4 is the amount of protein in the collected supernatant and washing fractions after co-immobilization. High immobilization yields of β-galactosidase (96.2%) and lysozyme (93.5%) were obtained.

Enzymatic activities of co-immobilized enzymes The activity of β-galactosidase towards its natural substrate lactose was assayed using a previously described method with a slight modification (10). After encapsulated β-galactosidase was rinsed sufficiently with distilled water to remove the P123 in the silica matrix, there suspended precipitate was allowed to stand for 5 min in PBS buffer (0.05 M, pH 7.0). Next, the hydrolytic activity of the encapsulated β-galactosidase was determined toward lactose (100 mM, pH 7.0) by combining 100 μL of diluted β-galactosidase and 900 μL of 100 mM lactose in 50 mM potassium phosphate buffer (pH 7.0) for 10 min at 37°C. The hydrolytic reaction was terminated by heating the mixture to 90°C for 2 min to quench the activity of the β-galactosidase. Next, the assay solution was centrifuged at 3500 × *g* for 3 min. Released D-glucose was determined from the absorbance at 540 nm using a glucose (GO) assay kit. Soluble β-galactosidase activity was determined using this protocol without centrifugation. One unit of β-galactosidase activity was defined as the amount of β-galactosidase that released 1 μmol of glucose per min under the defined conditions.

Assessment of lysozyme activity was conducted according to the Shugar method with alterations (25). Dried *M. lysodeikticus* powder was dispersed in 20 mL of PBS buffer (0.05 M, pH 7.0). Next, dilutions of lysozyme solution (1 ml) were added to 9 ml of bacterial solution at 37°C. A sample was withdrawn from the reaction mixture (1 mL), centrifuged at 1500 × *g* for 1 min to pellet the silica matrix, then the absorbance of the remaining cell suspension at 450 nm was measured using a Shimadzu UV-2550 spectrometer (Shimadzu, Kyoto, Japan). One unit of lysozyme activity was defined as the amount of lysozyme that caused a decrease in absorbance at 450 nm of 0.001 per min under these conditions.

Reusability The co-immobilized enzymes were tested in successive batches. The enzymatic activity of encapsulated β-galactosidase was determined based on the above mentioned lactose assay procedure. The hydrolytic reaction of 4-MU-β-$(GlcNAc)_3$ catalyzed by lysozyme was adopted to assess the reusability of bound lysozyme (26). The hydrolytic reaction was carried out in PBS buffer (0.05 M, pH 7.0) containing 0.03 mg/ml of 4-MU-β-$(GlcNAc)_3$ and 5 ml of appropriately diluted co-immobilized enzymes at 37°C for 20 min. Next, the reaction system was centrifuged at 1500 × *g* for 1 min and the fluorescence of the suspension at

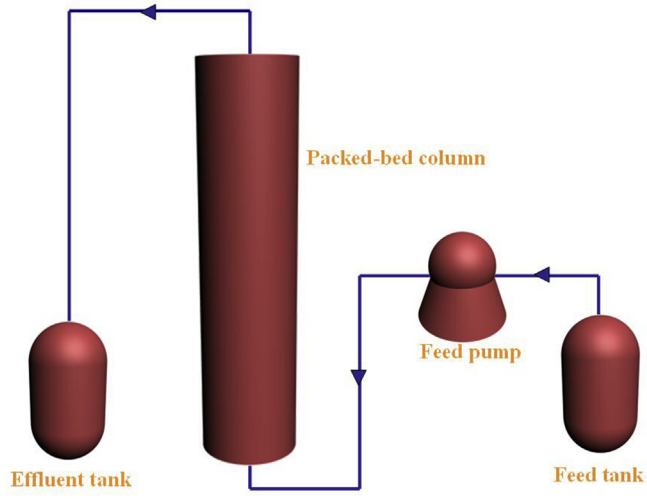

FIG. 1. The dual-functional continuous operation system.

460 nm was measured using a Perkin Elmer LS-55 fluorescence spectrometer (Perkin Elmer, Waltham, MA, USA). At the end of each batch run, co-immobilized enzyme matrix was centrifugally separated and washed three times with PBS buffer (0.05 M, pH 7.0). After washing, the matrix was resuspended in fresh assay buffer and incubated with fresh substrate for execution of the next cycle. This procedure was repeated to achieve ten runs for each tested matrix formulation.

Continuous system operation Co-immobilized enzymes (10.0 g) were packed in columns (packed volume, 16.0 ml) of suitable dimensions (2.0 cm × 10.0 cm). Next, skim milk was passed through the columns at different flow rates (6–60 ml h^{-1}) at 25°C. Lactose hydrolysis within the effluent was determined from the amount of glucose produced using a glucose (GO) assay kit. As for the antimicrobial assay, serial dilutions of effluent were poured into petri dishes containing agar medium and mixed with gentle stirring. Cultures were grown at 37°C for 48 h in order to obtain punctiform colonies. The survival ratio of cells was defined as the percentage of viable cells in suspensions relative to the total number of the cells in untreated milk.

Lactose (0.1 M) solution containing 0.001 M sodium azide was run through the packed-bed column under different flow rates at 25°C. The column was in operation for 60 days and the glucose concentration of the effluent was measured using the glucose (GO) assay kit every ten days.

Skim milk was passed through the column at a flow rate of 6 ml h^{-1} at 25°C for 30 days. Aliquots of effluent were withdrawn at regular intervals to measure the amount of glucose formed and the survival ratio of cells in the treated milk. In batch mode, properly diluted co-immobilized enzymes were incubated with skim milk at 25°C with stirring for 8 h in the batch system. Next, the mixture was centrifuged at 1500 × *g* for 1 min to determine the amount of glucose formed and the survival ratio of cells in the treated suspension. The collected co-immobilized enzymes were washed three times with PBS buffer (0.05 M, pH 7.0) and then stored at 4°C before being transferred into untreated skim milk the next day. This procedure was repeated until completion of 30 cycles.

Statistical analysis The data obtained in various studies was plotted using Origin 8.5 and expressed as (±) standard error. Each value represents the mean of three independent experiments implemented in duplicate, with average standard deviations <5%.

RESULTS AND DISCUSSION

Optimizing the encapsulation of β-galactosidase The specific activities for different amounts of encapsulated β-galactosidase were measured to determine the optimal enzyme amount. The experimental data confirmed that the specific activity of the encapsulated β-galactosidase significantly increased with an increase in the amount of added enzyme within the range of 0–0.6 g then slowly declined with further increases in enzyme amount from 0.6 to 2.0 g (Fig. 2A). The increase in specific activity was likely due to the increase of enzyme loading amount when the amount of added enzyme was less than 0.6 g. However, as the amount of added enzyme increased above 0.6 g, the surplus β-galactosidase brought about the diffusion limit of substrate and products, leading to subsequent decreases in specific activity. Therefore, 0.6 g was chosen as the optimal enzyme amount used in this study.

To obtain the optimal aging time, specific activities of encapsulated β-galactosidase were surveyed to study the effect of aging time on the specific activity of encapsulated β-galactosidase (Fig. 2B). Linear increases in specific activity had been observed with increasing aging time up to 72 h, while a slight decrease in activity was found with prolonged aging to 90 h. The reduction of aging time may cause instability of the silica skeleton in the host matrix that resulted in its collapse after extraction of the solvent and would thus negatively impact specific activity (27). On the other hand, if the aging time was too long, the pore volume of the host matrix tended to decrease to that of the corresponding xerogel, also causing reduction of specific activity (28). Therefore, 72 h was selected as the optimal aging time in this study.

N_2 adsorption/desorption isotherms After rinsing, N_2 adsorption/desorption isotherms of NH_2-silica and NH_2-silica-enzymes were measured to investigate the BJH pore diameter, BET surface area and pore volume of samples. N_2 adsorption/desorption isotherms of the samples exhibited narrow hysteresis loops of H_3 types, as classified by the International Union of Pure and Applied Chemistry (IUPAC) (29) (Fig. S1A and B). As shown in Table S1, higher BJH pore diameter, total pore volume and BET surface area of NH_2-silica were observed and are compared with corresponding values observed for NH_2-silica-enzymes.

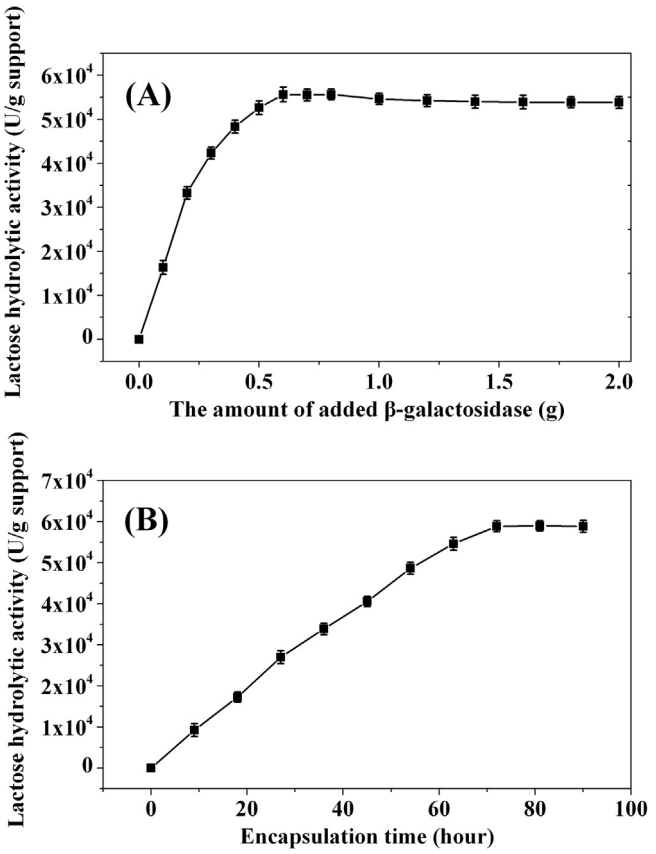

FIG. 2. (A) The effect of enzyme amount on encapsulation yield. Encapsulation conditions: PBS buffer, 0.05 M, pH 7.0; temperature, 4°C; β-galactosidase, 0–2.0 g; and aging time, 54 h. (B) The effect of the aging time. Encapsulation conditions: PBS buffer, 0.05 M, pH 7.0; temperature, 4°C; 0.6 g of β-galactosidase and aging times within a range of 9–90 h.

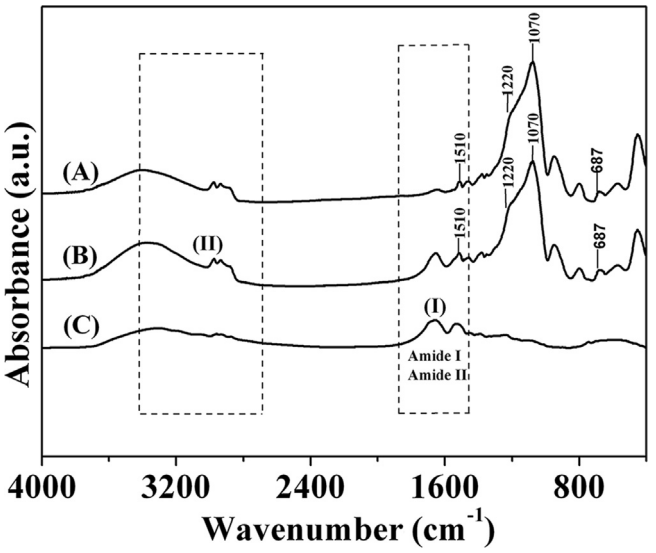

FIG. 3. FTIR spectra of the amino-functionalized silica matrix (A), encapsulated β-galactosidase (B) and β-galactosidase (C).

FTIR analysis As shown in Fig. 3, peaks around 1220 cm^{-1} and 1070 cm^{-1} corresponding to Si-O-Si stretch originating from the condensed silica skeleton could be found in curve A. However, absorbance of amino groups at 687 cm^{-1} and 1510 cm^{-1} displayed in curve B indicate successful incorporation of amino groups into the silica matrix. Meanwhile, the amide I and amide II infrared peaks of β-galactosidase in the range of 1500–1700 cm^{-1} (region I) could be observed in both curve C and in curve B; however, in curve B peaks corresponding to Si-O-Si stretch could also be seen (Fig. 3), confirming the existence of β-galactosidase within the amino-functionalized silica matrix. The broad peaks arising from amino groups at 2700–3400 cm^{-1} were observed in all curves (region II). As for curve A, the broad peaks in region II likely are due to amino groups in the silica matrix, while in curve C the broad peaks in the same region likely correspond to amino groups from β-galactosidase. As for curve B, the broad peaks in region II correspond to amino groups of both the silica matrix and β-galactosidase. After the cross linking of lysozyme was complete, a 2.73-fold decrease in peak area ratio between Si-O-Si to that of amide I for the co-immobilized enzymes was observed compared with the encapsulated β-galactosidase (Fig. S2), indicating the amido bond formation between lysozyme and amino-grafted silica carrier. The peak areas ratios were determined by the Gaussian modeling using origin 8.5 software (OriginLab Corporation, Northampton, MA, USA) (30).

Optimizing covalent immobilization of lysozyme Antibacterial activity depended on the concentration of lysozyme used within the concentration range of 0–2.0 mg/ml, where by antibacterial activity significantly increased with increase in lysozyme concentration within the range of 0–1.5 mg/ml (Fig. 4A). With further increase in concentration within the range of 1.5–2.0 mg/ml, the antibacterial activity of bound lysozyme reached a plateau, with the highest antibacterial activity observed at a lysozyme concentration of 2.0 mg/ml (Fig. 4A).

Effect of glutaraldehyde concentration Glutaraldehyde concentration is an important parameter that influences covalent binding of enzyme to the support surface (31). In this study, the relationship between glutaraldehyde concentration and antibacterial activity of bound lysozyme was examined within the glutaraldehyde concentration range of 0.02%–10.0%. It was observed that the antibacterial activity of bound lysozyme significantly increased in the concentration range of 0.02%–2.0%, which may be due to an increase in the amount of lysozyme bound to the amino-functionalized silica matrix (Fig. 4B). The antibacterial activity of bound lysozyme slightly decreased with further increase of glutaraldehyde concentration in the range 2%–10% (Fig. 4B). The slight final decrease of antibacterial activity might be due to the distortion of the lysozyme structure caused by extensive cross-linking by glutaraldehyde (32). Because the maximum antibacterial activity was observed at 2.0% glutaraldehyde, this glutaraldehyde concentration was chosen as the optimal reaction concentration in this study.

The effect of immobilization reaction time on bound lysozyme The influence of reaction time within the range of 1–15 h on the covalent immobilization process was investigated. The results demonstrated that the antibacterial activity of bound lysozyme did not obviously change in step with the extension of reaction time (Fig. 4C). Considering that the antibacterial activity of bound lysozyme at a reaction time of 6 h was slightly higher than

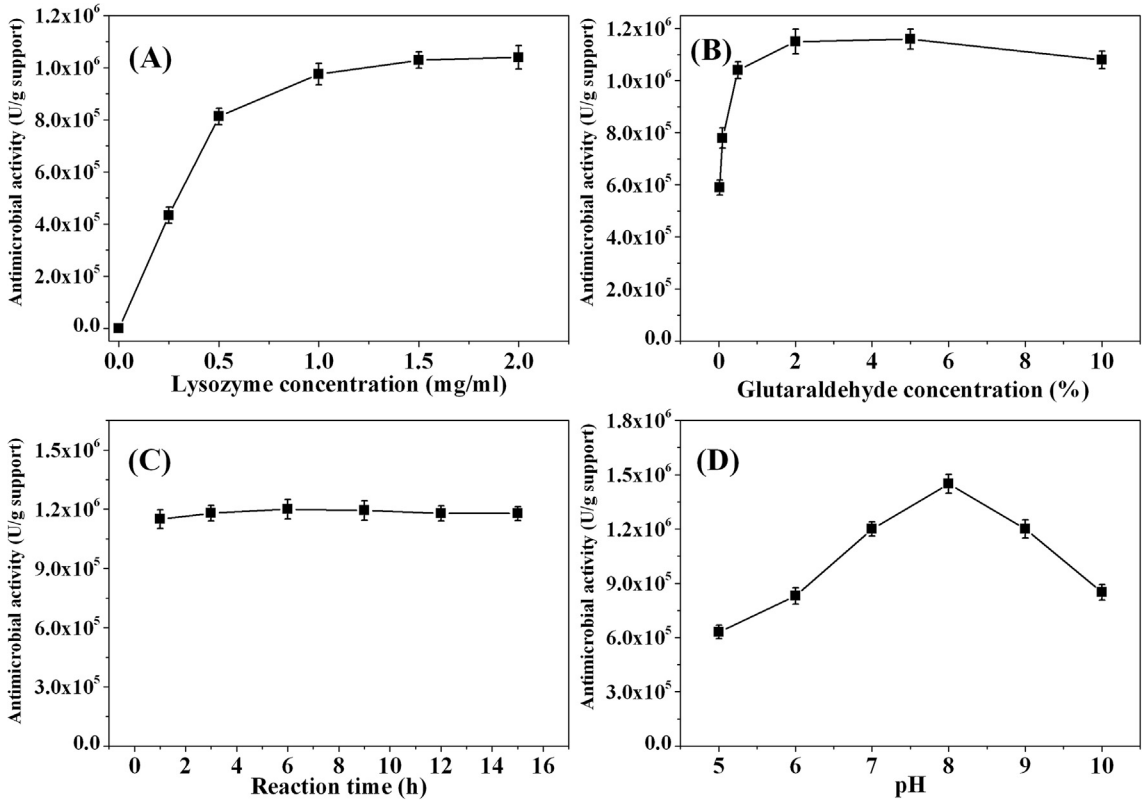

FIG. 4. (A) Effect of lysozyme concentration. Covalent binding conditions: PBS buffer, 0.05 M, pH 7.0; glutaraldehyde, 0.5%; lysozyme, 0–2.0 mg/ml; and reaction time, 12 h. (B) Effect of glutaraldehyde concentration. Covalent binding conditions: PBS buffer, 0.05 M, pH 7.0; lysozyme, 2.0 mg/ml; glutaraldehyde, 0.02%–10.0%; and reaction time, 12 h. (C) Effect of reaction time. Covalent binding conditions: PBS buffer, 0.05 M, pH 7.0; lysozyme, 2.0 mg/ml; glutaraldehyde, 2.0%; and reaction time, 1–15 h. (D) Effect of pH on coupling reaction. Covalent binding conditions: PBS buffer, 0.05 M, pH 5.0–10.0; lysozyme, 2.0 mg/ml; glutaraldehyde, 2.0%; and reaction time, 6 h.

that of the other sample times, the covalent linkage reaction between lysozyme and the amino-functionalized silica matrix was performed for 6 h in this study. In general, although ambient temperature had been used for glutaraldehyde immobilization of enzymes within 4 h or less (33,34), in this experiment the reactions were carried out at low temperature (4°C) to protect the enzymatic activity of encapsulated β-galactosidase and bound lysozyme. This lower temperature necessitated a longer immobilization reaction time (6 h), in agreement with published results (35).

The effect of pH on lysozyme immobilization reaction Generally speaking, the reaction of glutaraldehyde with enzymes is shown to be pH-dependent (31). In this study, the covalent immobilization of lysozyme was carried out for various phosphate buffer pH values (0.05 M, pH 5.0–9.0) and it was observed that the change of enzyme activities with pH exhibited a bell-shaped curve, with bound lysozyme exhibiting maximum enzyme activity in 0.05 M phosphate buffer at pH 8.0 in this study (Fig. 4D). At low pH (pH 5.0–7.0) or high pH (pH 9.0–10.0), enzyme inactivation led to decreased antibacterial activity.

Relative activities of free and immobilized enzymes As shown in Fig. 5A, bound lysozyme co-immobilized with β-galactosidase retained 96.3% of the antimicrobial activity of free lysozyme. The 3.7% loss in antimicrobial activity might be ascribed to the conformational change of lysozyme induced by the interaction between lysozyme and the host silica matrix (36). As for β-galactosidase, whether or not lysozyme was attached to the outer surface of the silica matrix, the hydrolytic activity of the encapsulated β-galactosidase in the silica matrix did not change (Fig. 5B), indicating that diffusion of lactose, galactose and galactose were not affected by the presence of lysozyme anchored to the outer part of the silica matrix. Indeed, encapsulated β-galactosidase in the silica matrix exhibited approximately 40% higher specific activity than did free enzyme, indicating that favorable conformers of β-galactosidase within the silica-based matrix induced by molecular imprinting technique could be retained and enriched via fish-in-net encapsulation (10).

Operational stability Operational stability of co-immobilized enzymes was investigated to assess their potential for practical use in the dairy industry. The results obtained in this study demonstrate that encapsulated β-galactosidase and bound lysozyme exhibited excellent reusability (Fig. 6), with encapsulated β-galactosidase maintaining almost 100% of its initial activity after ten cycles. Since the pore size of the amino functionalized silica matrix (2.7 nm) was smaller than the three-dimensional size of β-galactosidase (11 nm), leakage of β-galactosidase from the silica matrix was avoided. A slight loss in antimicrobial activity of bound lysozyme occurred during continuous operation, which might be ascribed to the slight leakage of bound lysozyme throughout the continuous batch mode.

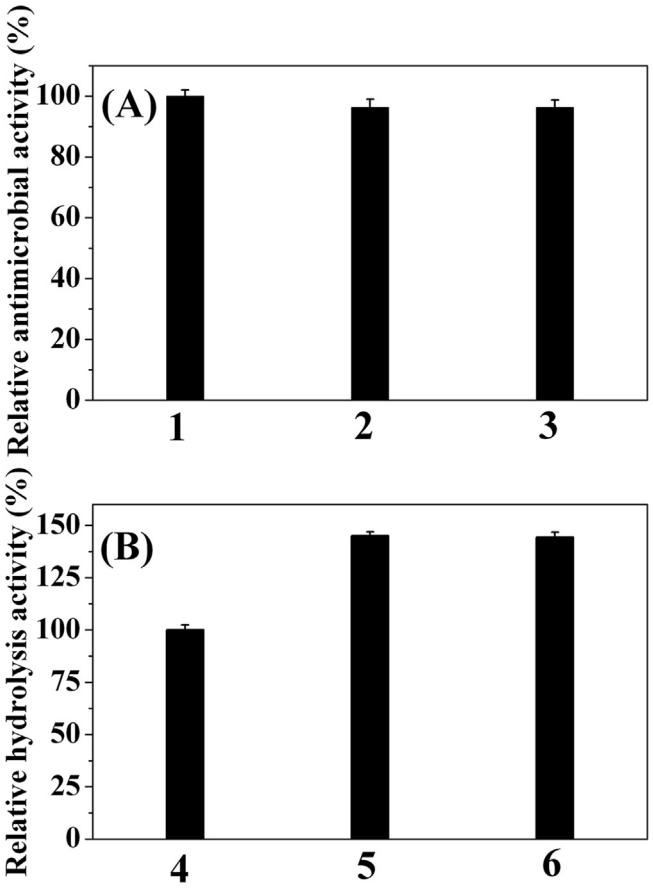

FIG. 5. Comparison of relative activities of immobilized and free enzymes. (A) 1, the relative activities of free lysozyme; 2, bound lysozyme without β-galactosidase; and 3, bound lysozyme with entrapped β-galactosidase. (B) 4, the relative activities of soluble β-galactosidase; 5, entrapped β-galactosidase without anchored lysozyme; and 6, co-immobilized enzymes. The specific activities of free lysozyme and β-galactosidase were used as controls (100%).

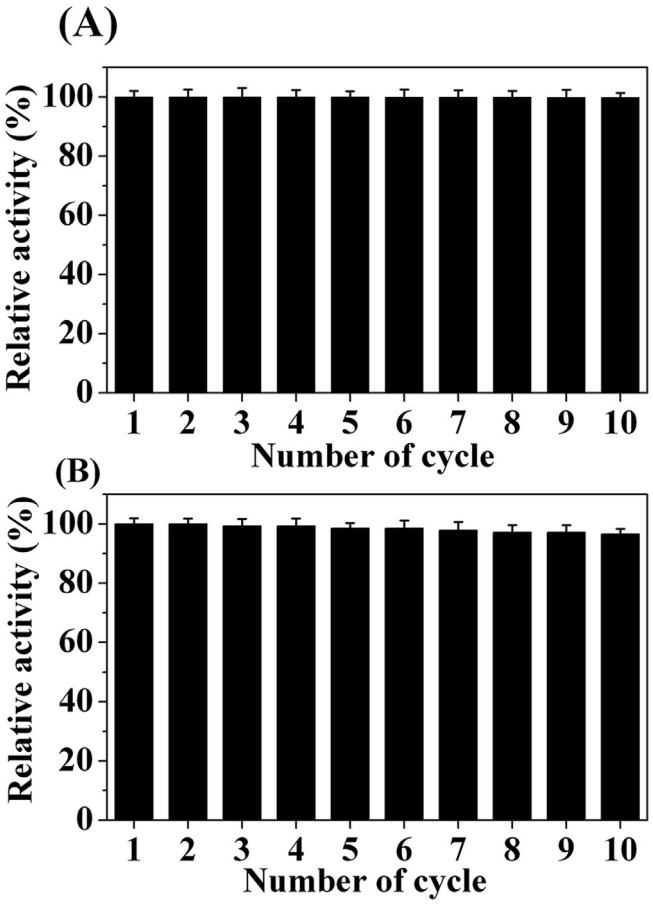

FIG. 6. (A) The operational stability of entrapped β-galactosidase. Reaction conditions for each run: PBS buffer, 0.05 M, pH 7.0; lactose solution, 100 mM; the properly diluted co-immobilized enzymes, 5 ml; and temperature, 37°C. (B) The operational stability of covalently immobilized lysozyme. Reaction conditions for each run: PBS buffer, 0.05 M, pH 7.0; 4-MU-β-$(GlcNAc)_3$, 0.03 mg/ml; properly diluted co-immobilized enzymes, 5 ml; and temperature, 37°C.

Continuous operation of the system The rate of lactose hydrolysis and the survival ratio of cells in skim milk were monitored at different cycle time points in a packed-bed column filled with co-immobilized enzymes. As shown in Fig. 7A, the rate of lactose hydrolysis dramatically increased with length of residence time with matrix. It was observed that 87.66% and 87.25% of lactose was hydrolyzed by co-immobilized enzymes in packed-bed columns when residence times were 160 min and 128 min, respectively, which conformed to the required amount of time observed previously for low-lactose milk production (37). Moreover, the survival ratio of cells significantly dropped as residence time increased, with co-immobilized enzymes exhibiting 15.75% and 19.44% cell survival rates after 160 min and 128 min treatment, respectively (Fig. 7B).

The extent of lactose hydrolysis was higher at a 6 mL h^{-1} flow rate than at a 7.5 mL h^{-1} flow rate, with 90.26% and 90.02% of lactose hydrolyzed by co-immobilized enzymes in a packed-bed reactor after 60 days of treatment cycles, respectively (Table 1). Overall, in skim milk 90.32% of the lactose hydrolytic rate and 15.35% of the microbial inactivation ratio were achieved after the first treatment cycle of the co-immobilized enzymes in the packed-bed column (Table 2). Notably, in the continuous mode the hydrolytic rate and microbial inactivation ratio remained stable for 30 days, with the good performance observed for the packed-bed reactor attributed to the high stability of co-immobilized enzymes. These results demonstrate that a packed-bed column filled with co-immobilized enzymes has great potential for industrial applications. In contrast, in the batch process, the lactose hydrolysis ratio of the co-immobilized enzymes gradually decreased to 74.31% and the microbial inactivation ratio increased to 20.02% after 30 days of treatment cycles (Table 2), with the slight loss of the co-immobilized enzymes resulting from repeated washing, centrifugation and decanting operations during the treatment process.

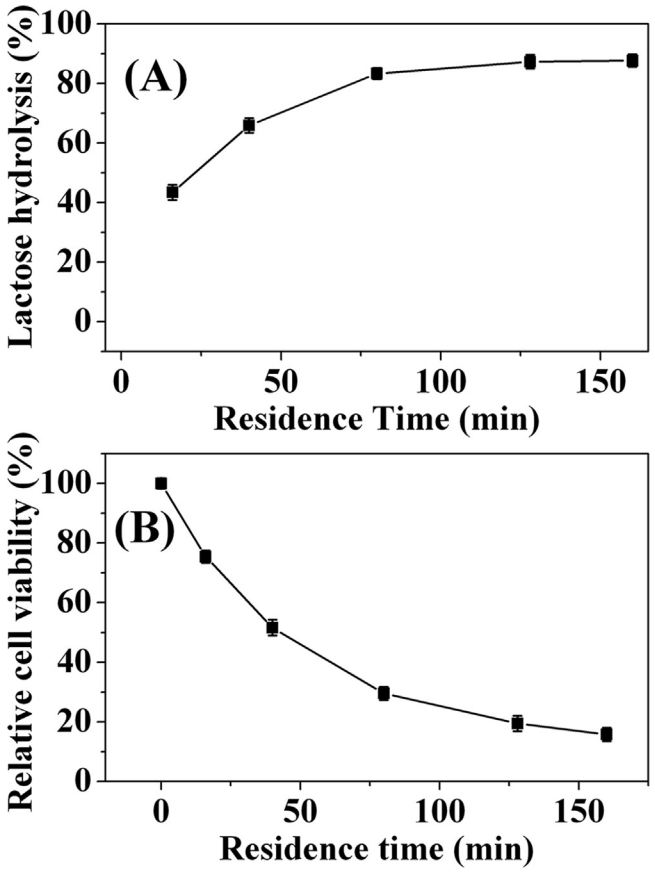

FIG. 7. Hydrolysis of lactose (A) and microbial inactivation (B) in skim milk treated with co-immobilized enzymes in a packed-bed column.

TABLE 1. Lactose hydrolysis (%) of co-immobilized enzymes in continuous packed-bed reactors at different flow rates.

Number of days	Flow rate	
	6 ml h^{-1}	7.5 ml h^{-1}
0	97.32 ± 1.11	96.89 ± 1.03
10	93.57 ± 1.01	93.25 ± 0.64
20	93.59 ± 0.56	92.61 ± 0.59
30	92.12 ± 1.05	92.63 ± 1.01
40	92.01 ± 0.78	91.35 ± 0.88
50	90.55 ± 0.68	90.43 ± 0.76
60	90.26 ± 1.06	90.02 ± 1.03

TABLE 2. Hydrolysis of lactose and inhibition of bacterial growth in slim milk treated in different modes within 30 days.

Number of days	Continuous mode		Batch mode	
	Lactose hydrolysis (%)	Relative cell viability (%)	Lactose hydrolysis (%)	Relative cell viability (%)
0	90.32 ± 1.11	15.35 ± 0.63	90.44 ± 0.57	15.75 ± 1.03
5	90.07 ± 1.01	15.59 ± 0.73	86.47 ± 0.91	16.89 ± 0.86
10	89.59 ± 0.56	15.68 ± 0.48	83.09 ± 1.16	17.73 ± 0.99
15	88.12 ± 1.05	15.80 ± 0.94	81.35 ± 0.78	18.02 ± 0.75
20	88.01 ± 0.78	15.77 ± 0.87	78.01 ± 0.38	19.26 ± 0.91
25	87.55 ± 0.68	16.23 ± 0.51	76.55 ± 0.54	19.80 ± 1.01
30	87.26 ± 1.06	16.56 ± 0.89	74.31 ± 0.77	20.02 ± 0.93

In this study, β-galactosidase was entrapped within an amino-grafted silica matrix employing TEOS and APTES silica sources. FTIR spectra verified the presence of β-galactosidase within the silica matrix. After β-galactosidase entrapment, covalent attachment of lysozyme to the surface of the silica matrix was achieved by glutaraldehyde fixation. Notably, host matrices loaded with the two enzymes exhibited good enzymatic activities and excellent reusability under continuous operation. Finally, the packed-bed column reactor loaded with co-immobilized enzymes offered a high lactose hydrolysis rate and microbial inactivation ratio in skim milk during 30 days of continuous operation. Indeed, during 60 days of continuous operation, the packed-bed column reactor still maintained good lactose hydrolysis performance. This work paves the way for the production of low lactose milk using silica matrix loaded with the two enzymes.

Supplementary data related to this article can be found at https://doi.org/10.1016/j.jbiosc.2018.07.009.

ACKNOWLEDGMENTS

This work was supported by the Jilin Province Innovation Platform of Straw Comprehensive Utilization Technology (Technology and Innovation Platform of Colleges and Universities of Jilin Province (2014) C-1), the 13th Five-Year scientific research Planning Project of the Education Department of Jilin Province (JJKH20170305KJ) and the PhD Scientific Research Start-up Fund Project of Jilin Agricultural University (201607).

References

1. **Jelen, P. and Tossavainen, O.:** Low lactose and lactose-free milk and dairy products-prospects, technologies and applications, Aust. J. Dairy Technol., **58**, 161–165 (2003).
2. **Cais-Sokolińska, D., Wójtowski, J., and Pikul, J.:** Lactose hydrolysis and lactase activity in fermented mixtures containing mare's, cow's, sheep's and goat's milk, Int. J. Food Sci. Technol., **51**, 2140–2148 (2016).

3. **Harju, M., Kallioinen, H., and Tossavainen, O.:** Lactose hydrolysis and other conversions in dairy products: technological aspects, Int. Dairy J., **22**, 104–109 (2012).
4. **Panesar, P. S., Panesar, R., Singh, R. S., Kennedy, J. F., and Kumar, H.:** Microbial production, immobilization and applications of β-D-galactosidase, J. Chem. Technol. Biotechnol., **81**, 530–543 (2006).
5. **Bahamondes, C., Wilson, L., Guzmán, F., and Illanes, A.:** Mathematical determination of kinetic parameters for assessing the effect of the organic solvent on the selectivity of peptide synthesis with immobilized α-chymotrypsin, J. Biosci. Bioeng., **124**, 618–622 (2017).
6. **Zhao, Z., Xie, X., Wang, Z., Tao, Y., Niu, X., Huang, X., Liu, L., and Li, Z.:** Immobilization of *Lactobacillus rhamnosus* in mesoporous silica-based material: an efficiency continuous cell-recycle fermentation system for lactic acid production, J. Biosci. Bioeng., **121**, 645–651 (2016).
7. **Kojima, T., Mizoguchi, T., Ota, E., Hata, J., Homma, K., Zhu, B., Hitomi, K., and Nakano, H.:** Immobilization of proteins onto microbeads using a DNA binding tag for enzymatic assays, J. Biosci. Bioeng., **121**, 147–153 (2016).
8. **Wei, C., Zhou, Y., Zhuang, W., Li, G., Jiang, M., and Zhang, H.:** Improving the performance of immobilized β-glucosidase using a microreactor, J. Biosci. Bioeng., **125**, 377–384 (2017).
9. **Chang, F., Xue, S., Xie, X., Fang, W., Fang, Z., and Xiao, Y.:** Carbohydrate-binding module assisted purification and immobilization of β-glucosidase onto cellulose and application in hydrolysis of soybean isoflavone glycosides, J. Biosci. Bioeng., **125**, 185–191 (2018).
10. **Wu, Z., Dong, M., Lu, M., and Li, Z.:** Encapsulation of β-galactosidase from Aspergillus oryzae based on "fish-in-net" approach with molecular imprinting technique, J. Mol. Catal. B Enzym., **63**, 75–80 (2010).
11. **Boor, K. J., Wiedmann, M., Murphy, S., and Alcaine, S.:** A 100-Year Review: microbiology and safety of milk handling, J. Dairy Sci., **100**, 9933–9951 (2017).
12. **Schindler, M., Assaf, Y., Sharon, N., and Chipman, D. M.:** Mechanism of lysozyme catalysis: role of ground-state strain in subsite D in hen egg-white and human lysozymes, Biochemistry, **16**, 423–431 (1977).
13. **Lesnierowski, G., Kijowski, J., and Cegielska-Radziejewska, R.:** Ultrafiltration-modified chicken egg white lysozyme and its antibacterial action, Int. J. Food Sci. Technol., **44**, 305–311 (2009).
14. **Cannarsi, M., Baiano, A., Sinigaglia, M., Ferrara, L., Baculo, R., and Del Nobile, M. A.:** Use of nisin, lysozyme and EDTA for inhibiting microbial growth in chilled buffalo meat, Int. J. Food Sci. Technol., **43**, 573–578 (2008).
15. **Shahani, K., Harper, W., Jensen, R., Parry, R., and Zittle, C.:** Enzymes in bovine milk: a review, J. Dairy Sci., **56**, 531–543 (1973).
16. **Alderton, G., Ward, W., and Fevold, H.:** Isolation of lysozyme from egg white, J. Biol. Chem., **157**, 43–58 (1945).
17. **Li, H., Li, S., Tian, P., Wu, Z., and Li, Z.:** Prevention of bacterial contamination of a silica matrix containing entrapped β-galactosidase through the action of covalently bound lysozymes, Molecules, **22**, 377 (2017).
18. **Li, Y. M., Tan, A. X., and Vlassara, H.:** Antibacterial activity of lysozyme and lactoferrin is inhibited by binding of advanced glycation–modified proteins to a conserved motif, Nat. Med., **1**, 1057–1061 (1995).
19. **Besharati Vineh, M., Saboury, A. A., Poostchi, A. A., Rashidi, A. M., and Parivar, K.:** Stability and activity improvement of horseradish peroxidase by covalent immobilization on functionalized reduced graphene oxide and biodegradation of high phenol concentration, Int. J. Biol. Macromol., **106**, 1314–1322 (2018).
20. **Kumar, S., Haq, I., Prakash, J., and Raj, A.:** Improved enzyme properties upon glutaraldehyde cross-linking of alginate entrapped xylanase from *Bacillus licheniformis*, Int. J. Biol. Macromol., **98**, 24–33 (2017).
21. **Hosseini, S. H., Hosseini, S. A., Zohreh, N., Yaghoubi, M., and Pourjavadi, A.:** Covalent immobilization of cellulase using magnetic poly(ionic liquid) support: improvement of the enzyme activity and stability, J. Agric. Food Chem., **66**, 789–798 (2018).
22. **Walt, D. R. and Agayn, V. I.:** The chemistry of enzyme and protein immobilization with glutaraldehyde, TrAC, Trends Anal. Chem., **13**, 425–430 (1994).
23. **Tran, D. N. and Balkus, K. J.:** Perspective of recent progress in immobilization of enzymes, ACS Catal., **1**, 956–968 (2011).
24. **Bradford, M. M.:** A rapid and sensitive method for the quantitation of microgram quantities of protein utilizing the principle of protein-dye binding, Anal. Biochem., **72**, 248–254 (1976).
25. **Shugar, D.:** The measurement of lysozyme activity and the ultra-violet inactivation of lysozyme, Biochim. Biophys. Acta, **8**, 302–309 (1952).
26. **Sang, L.-C. and Coppens, M.-O.:** Effects of surface curvature and surface chemistry on the structure and activity of proteins adsorbed in nanopores, Phys. Chem. Chem. Phys., **13**, 6689–6698 (2011).
27. **Pierre, A. C.:** The sol-gel encapsulation of enzymes, Biocatal. Biotransform., **22**, 145–170 (2004).
28. **Gill, I. and Ballesteros, A.:** Encapsulation of biologicals within silicate, siloxane, and hybrid Sol–Gel Polymers: an efficient and generic approach, J. Am. Chem. Soc., **120**, 8587–8598 (1998).
29. **Tompsett, G., Krogh, L., Griffin, D., and Conner, W.:** Hysteresis and scanning behavior of mesoporous molecular sieves, Langmuir, **21**, 8214–8225 (2005).
30. **Marshall, I., Bruce, S. D., Higinbotham, J., MacLullich, A., Wardlaw, J. M., Ferguson, K. J., and Seckl, J.:** Choice of spectroscopic lineshape model affects metabolite peak areas and area ratios, Magn. Reson. Med., **44**, 646–649 (2000).
31. **Habeeb, A. F. S. A. and Hiramoto, R.:** Reaction of proteins with glutaraldehyde, Arch. Biochem. Biophys., **126**, 16–26 (1968).
32. **Migneault, I., Dartiguenave, C., Bertrand, M. J., and Waldron, K. C.:** Glutaraldehyde: behavior in aqueous solution, reaction with proteins, and application to enzyme crosslinking, Biotechniques, **37**, 790–802 (2004).
33. **Krogh, T. N., Berg, T., and Højrup, P.:** Protein analysis using enzymes immobilized to paramagnetic beads, Anal. Biochem., **274**, 153–162 (1999).
34. **Tomer, S., Dorsey, J. G., and Berthod, A.:** Nonionic micellar liquid chromatography coupled to immobilized enzyme reactors, J. Chromatogr. A, **923**, 7–16 (2001).
35. **Kennedy, J. F. and Cabral, J. M. S.:** Immobilized enzymes, pp. 253–391, in: Scouten, W. H. (Ed.), Solid phase biochemistry: analytical and synthetic aspects. John Wiley & Sons, New York (1983).
36. **Secundo, F.:** Conformational changes of enzymes upon immobilisation, Chem. Soc. Rev., **42**, 6250–6261 (2013).
37. **Paige, D. M., Bayless, T. M., Huang, S. S., and Wexler, R.:** Lactose hydrolyzed milk, Am. J. Clin. Nutr., **28**, 818–822 (1975).